Development 134, 4506 (2007) doi:10.1242/dev.02887

Notch2, but not Notch1, is required for proximal fate acquisition in the mammalian nephron

Hui-Teng Cheng, Mijin Kim, M. Todd Valerius, Kameswaran Surendran, Karin Schuster-Gossler, Achim Gossler, Andrew P. McMahon and Raphael Kopan

There was an error published in *Development* **134**, 801-811.

On p. 802, Engleka et al. (2005) was mistakenly cited. The text should have read 'We crossed *Pax3-cre*$^{tg/+}$;*N2*$^{f/+}$ (*floxed Notch2*)/+ males (Li et al., 2000) to *N2*$^{f/f}$ females to obtain *Pax3-cre*$^{tg/+}$;*N2*$^{f/f}$ embryos or pups'.

The authors apologise to readers for this mistake.

Development 134, 801-811 (2007) doi:10.1242/dev.02773

Notch2, but not Notch1, is required for proximal fate acquisition in the mammalian nephron

Hui-Teng Cheng[1], Mijin Kim[1], M. Todd Valerius[2], Kameswaran Surendran[1], Karin Schuster-Gossler[3], Achim Gossler[3], Andrew P. McMahon[2] and Raphael Kopan[1,*]

The Notch pathway regulates cell fate determination in numerous developmental processes. Here we report that Notch2 acts non-redundantly to control the processes of nephron segmentation through an Rbp-J-dependent process. Notch1 and Notch2 are detected in the early renal vesicle. Genetic analysis reveals that only Notch2 is required for the differentiation of proximal nephron structures (podocytes and proximal convoluted tubules) despite the presence of activated Notch1 in the nuclei of putative proximal progenitors. The inability of endogenous Notch1 to compensate for Notch2 deficiency may reflect sub-threshold Notch1 levels in the nucleus. In line with this view, forced expression of a γ-secretase-independent form of Notch1 intracellular domain drives the specification of proximal fates where all endogenous, ligand-dependent Notch signaling is blocked by a γ-secretase inhibitor. These results establish distinct (non-redundant), instructive roles for Notch receptors in nephron segmentation.

KEY WORDS: Notch, Rbp-J, Wnt4, Proximal tubule, Podocytes, Nephron segmentation, Mouse

INTRODUCTION

The kidney is an essential excretory organ that maintains osmotic, acid-base and electrolyte equilibrium. The crucial importance of the kidney makes it a common target of systemic diseases, developmental syndromes and drug toxicity. The functional unit of the mammalian kidney is the nephron; each nephron patterns along a proximodistal axis into distinct functional domains; proximal to distal there are the glomerulus, proximal tubule, loop of Henle and distal tubule. How this crucial regional structure is established is not well understood.

Nephrons form from a simple epithelial precursor, the renal vesicle (RV), itself a product of a Wnt-induced mesenchymal-to-epithelial transition in the outer cortex (Carroll et al., 2005). The RV begins a series of molecular changes reflected by a stereotyped set of morphological and molecular changes. Morphologically, the RV transitions through a comma-shaped, then an S-shaped body stage before fusing with the adjacent epithelium of the ureteric bud (UB)-derived collecting duct system to establish a continuous tubular network. Asymmetric expression of Brn-1 (Pou3f3 – Mouse Genome Informatics) (Nakai et al., 2003), E-cadherin (cadherin-1 – Mouse Genome Informatics) and cadherin 6 (Cho et al., 1998) provide some of the first evidence for polarization of the proximodistal axis (the future glomerulo-collecting duct axis), but it is not until the S-shaped body stage that the future proximodistal axis is readily distinguishable. At this time, Pax2 is highly expressed within the distal portion of the S-shaped body, including the region that fuses to the UB. Podocyte precursors, which differentiate into glomerular podocytes, reside in the proximal limb of the S-shaped body (the visceral epithelial cells) and express high levels of Wilms' tumor-1 (Wt1) (Kreidberg et al., 1993). Adjacent to the podocyte in the cleft of the proximal limb, the vascular endothelial network of the future glomerular filtration apparatus starts to assemble. Although fate-mapping studies have not addressed the contribution of distinct regions within the S-shaped body to the future nephron, a cadherin-6-positive domain that lies between the presumptive podocytes and the Pax2(+) distal tubule progenitors is likely to give rise, at least in part, to the proximal convoluted tubule, a *Lotus tetragonolobus* lectin (LTL) (Laitinen et al., 1987) -binding epithelium in the mature nephron first visible at embryonic day (E) 14.5-15.5 in the mouse. The process of nephron formation continues at the periphery of the mouse kidney up to postnatal day 7; newborn kidneys thus contain nephrons at all stages of development.

Previous work examining the expression of Notch pathway components (Chen and Al-Awqati, 2005; Leimeister et al., 2003; Piscione et al., 2004) and modulating Notch signaling (Cheng et al., 2003; Wang et al., 2003) supported the argument for a Notch pathway activity in mammalian nephrogenesis. Notch genes encode single-transmembrane receptors that mediate short-range communication between cells. Receptor binding to ligand expressed on adjacent cells triggers the shedding of its extracellular domain and the subsequent cleavage of the transmembrane domain by the enzyme γ-secretase (for a review, see Mumm and Kopan, 2000). On γ-secretase-mediated proteolysis, the Notch intracellular domain (N1-ICD or N2-ICD) is released and translocates to the nucleus, where it associates with a DNA-bound REL-like protein (Cbf1/Rbp-J in vertebrates; Rbpsuh – Mouse Genome Informatics) and promotes transcription of its targets (Fryer et al., 2004; Lubman et al., 2004). In mammals, four Notch homologs (*Notch1-4*) and at least five ligands [jagged 1 (Jag1), Jag2, delta-like 1 (Dll1), Dll3 and Dll4] mediate these signaling events.

Notch1, *Notch2*, *Dll1* and *Jag1* mRNA are detected in the RV and its derivative; the expression domain of *Notch1* partially overlaps with *Notch2* in the S-shaped body (Chen and Al-Awqati, 2005). Notch2 and Jag1 are also expressed in the collecting duct. Humans haploinsufficient for jagged 1 (Li et al., 1997) are prone to Alagille syndrome, one symptom of which can result in the development of renal abnormalities (McCright, 2003; Piccoli and Spinner, 2001), whereas abnormal glomerulogenesis is observed when Notch2 activity is reduced (McCright et al., 2001). *Notch3* expression has

[1]Department of Molecular Biology and Pharmacology and Department of Medicine at Washington University School of Medicine, 660 South Euclid Avenue, Campus Box 8103, St Louis, MO 63110, USA. [2]Department of Molecular and Cellular Biology, Harvard University, 16 Divinity Avenue, Cambridge, MA 02138, USA. [3]Institute for Molecular Biology OE5250, Medizinische Hochschule Hannover, Carl-Neuberg-Str. 1 D-30625 Hannover, Germany.

*Author for correspondence (e-mail: kopan@wustl.edu)

Accepted 5 December 2006

been reported in the distal portion of the S-shaped body (Piscione et al., 2004); however, a *lacZ* knockin into the Notch3 locus indicates that only the glomerulus and blood vessels may express Notch3 (H.-T.C. and R.K., unpublished).

To date, no specific study has addressed the regional-specific action of the Notch pathway in nephron patterning, although the general, organ-wide inhibition of γ-secretase activity suggested that Notch activity is likely to be important, as podocytes and proximal tubules are lost when γ-secretase activity is abolished (Cheng et al., 2003; Wang et al., 2003). However, the observed phenotypes cannot be unequivocally attributed to loss of Notch signaling due to the existence of multiple other substrates of γ-secretase.

Here we have addressed the specific function of *Notch1* and *Notch2* by tissue-specific modulation of their activity. These studies reveal distinct roles for *Notch1* and *Notch2* in nephron development. Notch2 activity is essential for patterning of the proximal regions of the nephron. However, although *Notch1* is normally activated, and when overactivated is capable of proximalizing the nephron, it is not sufficient for the development of proximal cell fates. Thus, local activation of Notch2 during renal tubule morphogenesis is a central determinant of segmented pattern in the mammalian nephron.

MATERIALS AND METHODS

Notch2, Rbp-J and Notch1 mutant animals

We crossed *Pax3-cre$^{tg/+}$;N2$^{f/+}$* (*floxed Notch2*)/+ males (Engleka et al., 2005) to *N2$^{f/f}$* females to obtain *Pax3-cre$^{tg/+}$; N2$^{f/f}$* embryos or pups. We crossed *Pax2-cre$^{tg/+}$; N1$^{\Delta 1/+}$* (heterozygote for a null allele) (Conlon et al., 1995) males to *N1$^{f/f}$* females to produce *Pax2-cre$^{tg/+}$; N1$^{f/\Delta 1}$* embryos. *Pax2-cre$^{tg/+}$;Rbp-J$^{f/+}$* (Ohyama and Groves, 2004; Tanigaki et al., 2002) males were crossed with *Rbp-J$^{f/f}$* females to produce *Pax2-cre$^{tg/+}$; Rbp-J$^{f/f}$* embryos. Using the same scheme, we also generated *Pax2-cre$^{tg/+}$; N2$^{f/f}$* pups, which had the same phenotype as *Pax3-cre$^{tg/+}$; N2$^{f/f}$ pups*. In some cases, we analyzed *Pax2-cre$^{tg/+}$; N1$^{f/\Delta 1}$; Dll-1^{lacZ}* embryos (Hrabe de Angelis et al., 1997).

Six2-GFP::Cre males were crossed to *Rosa^{Notch}* (Notch1 intracellular domain) (Murtaugh et al., 2003) females to obtain *Rosa^{Notch}/+; Six2-GFP::Cre$^{tg/+}$* embryos. All mice used in this study were maintained on mixed backgrounds. Embryos were genotyped by standard PCR protocol. Noon of the day on which a vaginal plug was scored was designated as E0.5. The day when pups were born was designated as their first postnatal day (P1).

Generation of Notch1$^{-/-}$ ↔ wild-type chimeric embryos

The procedure is described in detail in Hadland et al. (Hadland et al., 2004). Briefly, compound heterozygotes for the Rosa26 locus and N1$^{\Delta 1}$ were crossed, blastocysts removed and cultured. LacZ-expressing control and Notch1-deficient embryonic stem (ES) cells were derived from Rosa26/+ and *N$^{\Delta 1/\Delta 1}$*; Rosa26/+ embryos, respectively. ES cells with normal karyotype were then injected into E3.5 wild-type CD1 blastocysts, which were then transferred into the uterus of pseudopregnant CD1 females. Whole-mount β-galactosidase (β-gal) staining (described below) was performed on the kidneys harvested from embryos at E16.5, before paraffin-embedded sectioning.

Metanephric organ culture

Mouse metanephric organ culture was performed as described by Rogers et al. (Rogers et al., 1991). Briefly, kidneys were removed from E12.5 mouse embryos and cultured on transwell filters (Falcon, pore size 1 μm) at an air-fluid interface in a serum-free medium consisting of equal volumes of Dulbecco's modified Eagle medium and Ham's F12 medium containing 25 mmol/l HEPES, sodium bicarbonate (1.1 mg/ml), 10 nmol/l $Na_2SeO_3.5H_2O$, 10^{-11} M prostaglandin E1, and iron-saturated transferrin (5 μg/ml). Medium was refreshed every day and the metanephroi were cultured for as long as 6 days.

Histology and immunohistochemistry

The kidneys or the cultured explants were fixed in Bouin's fixative or in 4% paraformaldehyde (PFA) [for LTL and 5-Bromo-2′-deoxyuridine (BrdU) analysis], embedded in paraffin and sectioned at 5 μm. The sections were then stained with Hematoxylin and Eosin (H&E) for histological analysis. For immunohistochemistry, the sections were boiled in Trilogy (Cell Marque) for antigen retrieval. The antibodies and the lectins were diluted as follows: rabbit anti-mouse cadherin 6 (1:300; kindly provided by Dr Dressler) (Cho et al., 1998), Ck8 (TROMA1; 1:10; Developmental Studies Hybridoma Bank), E-cadherin (1:1000; Transduction Labs), Jag1 (1:200; Santa Cruz), N-Cam (1:300, Sigma), Pax2 (1:200; Covance), Wt1 (1:100, Santa Cruz), synaptopodin (1:40, gift from Dr P. Mundel), laminin a1 and fluorescein isothiocyanate-conjugated LTL (1:100; Vector Labs). Hoechst (0.5 μg/ml, Sigma) was used for nuclear staining. Fluorescein- and Cy3-conjugated anti-IgG corresponding to the species of the primary antibodies was used to visualize the antigen. For cadherin 6, E-cadherin and Jag1, we used horseradish peroxidase (HRP)-conjugated IgG followed by tyramide-conjugated FITC or Cy3 for better results. For Notch1 detection, metanephroi were fixed in Bouin's fixative after 6 days in organ culture, dehydrated and embedded in paraffin wax. Sections (7 μm) were boiled in Trilogy for antigen retrieval, pre-blocked with PBS supplemented with 1% BSA, 0.2% skimmed milk, and 0.3% Triton X-100. A rabbit primary Notch 1 antibody (1:200, abcam ab27526) was used, followed by a biotinylated anti-rabbit IgG (1:3000). The Vectastain ABC kit (Vector Laboratory, Inc) and tyramide-conjugated Cy3 (TSA-Plus Cyanine 3, PerkinElmer, 1:100) were used to detect the signal.

To detect cleaved Notch1 in metanephroi, the following modified method was used. After incubation of the primary antibody V1744 (1:500, Cell Signaling Technology, a division of New England Biolabs), the sections were treated with HRP-conjugated anti-rabbit IgG (1:1000; Jackson ImmunoResearch), tyramide-conjugated FITC (NEN, PerkinElmer; 1:1000), and then HRP-conjugated anti-fluorescein antibody. The antigen was then visualized with tyramide-conjugated Cy3 (Cy3 Plus, NEN; 1:400).

Detection of Lim1 was done with anti-Lim1 antibody (Chemicon International) (Karavanov et al., 1996) with slight modification to the manufacturer's protocol. The kidney was fixed in MEMFA (MOPS 0.1 mol/l pH 7.4, EGTA 2 mmol/l, MgSO4 1 mmol/l, formaldehyde 3.7%) for 1 hour before embedding in paraffin. Rehydrated sections were boiled in Trilogy (Cell Marque) for antigen retrieval, and incubated with anti-Lim1 antibody at 5 ng/ml (1:200 of stock). To visualize the antigen, it is necessary to apply HRP-conjugated anti-rabbit IgG followed by tyramide-conjugated Cy3. This allows double staining with other primary rabbit antibodies like anti-Pax2.

For whole-mount staining, metanephroi were fixed in 4% PFA, washed in PBS and incubated in the blocking solution (MABT: 100 mmol/l maleic acid pH 7.5, 150 mmol/l NaCl, 0.1% Tween-20; plus 2% Blocking Reagent; Boehringer Mannheim) for one hour before adding anti-Ck8 antibody (1:10) for overnight incubation at room temperature. After extensive wash in MABT, the specimen was incubated with the Cy3-conjugated anti-rat IgG (1:1000). After this step, the metanephroi were incubated with FITC-LTL (1:200) for 1 hour at room temperature and then washed by PBS.

β-gal staining to detect LacZ activity

The kidneys were fixed in 4% PFA for 2 hours before whole-mount β-gal staining at room temperature overnight. The specimens were embedded in paraffin, sectioned and stained with antibody and/or counterstained with diluted Hematoxylin or Nuclear Fast Red (Vector Laboratories). After incubation with the primary antibody or FITC-conjugated LTL, the sections were treated with HRP-conjugated IgG or anti-FITC antibody followed by color development using diaminobenzidine tetrahydrochloride (DABT) as substrate.

Quantification of BrdU-labeling of cells

BrdU solution containing 5-Fluoro-2′-deoxyuridine (10% of the BrdU concentration) was injected intraperitoneally in pregnant mice 2 to 3 hours before kidney harvest. The samples were prepared and sectioned as described above before being incubated with mouse anti-mouse BrdU antibody (1:200) (Becton and Dickinson). It was visualized by Cy3 following HRP-conjugated IgG incubation. The sections were then subjected to staining with another antibody (Jag1 or Pax2) and then Hoechst nuclear stain. The single-color images were merged into one RGB file magnified in Adobe Photoshop. For BrdU-labeled Pax2 cells, we counted the number of BrdU-stained Pax2-expressing cells and the number of Pax2-

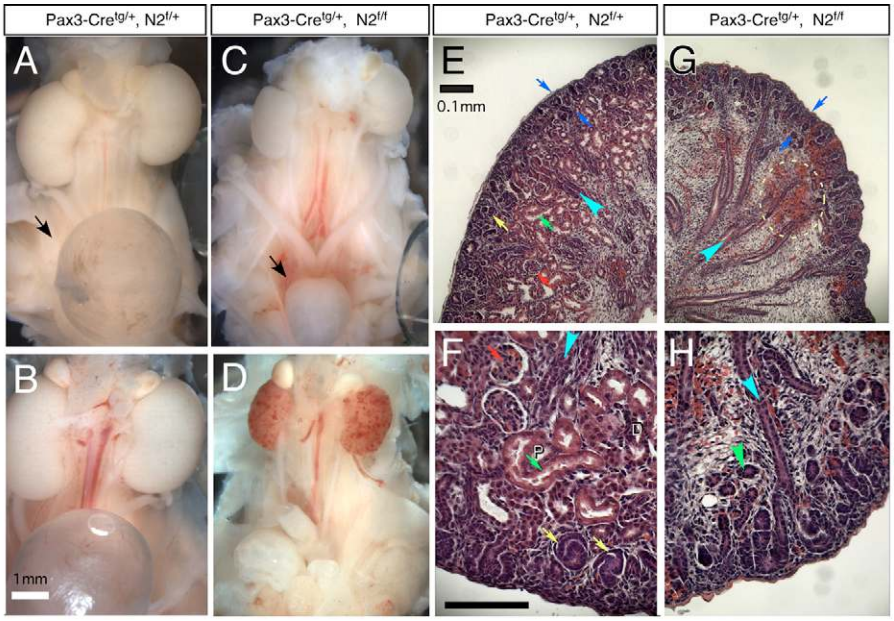

Fig. 1. Loss of *Notch2* causes hypoplastic kidneys that do not develop glomeruli, proximal tubules or S-shaped bodies. (**A-D**) The urinary system from postnatal day 1 and day 2 wild-type (A,B) or mutant (C,D) animals. Note the size difference of the urinary bladder (arrow in A and C). The mutant animals show spotty hemorrhage on the kidneys before they die on postnatal day 2 (D). (**E-H**) Histology of day 2 kidneys from wild type (E,F) and mutant (G,H) stained with H&E. The wild-type genotype is *Pax3-cre$^{tg/+}$; N2$^{f/+}$*; the mutant genotype is *Pax3-cre$^{tg/+}$; N2$^{f/f}$*. Blue arrows flank the nephrogenic zone; green arrow, proximal tubule; green arrowhead, presumptive renal tubule in mutant; red arrow, glomerulus; yellow arrow, S-shaped body; turquoise arrowhead, collecting duct; D, distal tubule; P, proximal tubule. Scale bars: 1 mm in A-D; 0.1 mm in E-H.

expressing cells within the Pax2-expressing RVs or early nephrons from one wild-type and one mutant kidney (19 RVs or early nephrons from each sample; each sample contains multiple sections). The data were presented as percentage of BrdU-positive Pax2 cells within the Pax2-expressing cells. For BrdU labeling index of Jag1 cells, sections from three different wild-type and three different mutant kidneys were included and 15 Jag1 clusters were counted in each kidney sample. Within each cluster we counted the number of BrdU-stained Jag1-expressing cells and the number of Jag1-expressing cells; and calculated the percentage of BrdU-labeled Jag1 cells in the Jag1-expressing cells. Student's *t*-test was used in the first comparison, and one-way ANOVA in the second comparison. $P<0.01$ was considered statistically significant.

In situ hybridization

Briefly, kidney samples were fixed in 4% PFA in PBS for 24 hours at 4°C and processed for OCT embedding. Frozen blocks were sectioned at 16 μm thickness and air dried. Slides were post-fixed in 4% PFA for 10 minutes, followed by three PBS washes, 3 minutes each. Slides were treated with Proteinase K, acetylated and rinsed and dehydrated before use. Digoxigenin-labeled riboprobes were made and column purified according to the manufacturer's instructions (Roche Applied Science). Hybridization was performed in a humidified chamber with a 200 μl probe and a parafilm coverslip at 68°C overnight. After hybridization, non-specific signal was removed by SSC washes and RNaseA digestions (detailed protocol is available upon request). Slides were then washed in MBST (100 mmol/l maleic acid, 150 mmol/l NaCl, 0.1% Tween-20, pH to 7.5) and blocked with 5% heat inactivated sheep serum (HISS) in 2% BMB (Roche Applied Science) in MBST, before adding anti-digoxigenin-AP antibody (1:4000 dilution) in 1% HISS, 2% BMB in MBST and incubated overnight in a humidified chamber at 4°C. Following extensive washes, signal was developed using BM Purple for 1 to 6 days in a humidified chamber at room temperature.

RESULTS

Conditional deletion of *Notch2* in the kidney causes complete loss of glomeruli and proximal tubules

To investigate the in vivo function of Notch receptors during nephrogenesis, we employed a Cre-mediated knockout strategy to disrupt these genes in the kidney mesenchyme using the *Pax3-cre* line (Li et al., 2000), which induces recombination in the metanephric mesenchyme (Grieshammer et al., 2005; Perantoni et al., 2005). Kidneys from *Pax3-cre$^{tg/+}$*; *Rosa26R$^{tg/+}$* embryos (Soriano, 1999) display LacZ expression in all metanephric mesenchyme-derived tissues, including comma- and S-shaped body and stromal tissue, while the UB derivatives remain unlabeled. The early and broad recombinase activity assures an early and complete recombination of alleles that is specific to the mesenchymal compartment and their epithelial derivatives (see Fig. S1A,B in the supplementary material) (see also Grieshammer et al., 2005; Perantoni et al., 2005).

Viable, normal *Pax3-cre$^{tg/+}$; N2$^{f/f}$* newborns were obtained at Mendelian ratios (data not shown). However, despite feeding successfully (data not shown), *Pax3-cre$^{tg/+}$; N2$^{f/f}$* animals died 24 to 48 hours after birth. Gross anatomical examination revealed that *Pax3-cre$^{tg/+}$; N2$^{f/f}$* had smaller kidneys than *Pax3-cre$^{tg/+}$; N2$^{f/+}$* siblings (Fig. 1A-D), and a small bladder suggested failure to produce urine (black arrows, Fig. 1A,C). During postnatal day 2 (P2), Notch2-deficient kidneys appeared to have lost vascular integrity (Fig. 1D). We observed hemorrhage into the interstitial spaces in *Pax3-cre$^{tg/+}$; N2$^{f/f}$* P1 kidney (Fig. 1G, circle). The renal pelvis was collapsed, the papilla was flattened (see Fig. S2A,B in the supplementary material) and the collecting ducts (turquoise arrow, Fig. 1E-H) were less extensively branched than those of wild-type or heterozygote *Pax3-cre$^{tg/+}$; N2$^{f/+}$* littermates, even though *N2$^{f/f}$* remains intact in the collecting duct network of the mutant. The nephrogenic zone, where the nephron initiating mesenchymal-to-epithelial transition takes place, appeared similar in thickness in both heterozygote and mutant kidneys (blue arrows, Fig. 1E,G), indicating a normal progression of the epithelialization process. By contrast, S-shaped bodies (yellow arrows), convoluted renal epithelia (green arrows) and glomeruli (red arrows), were not histologically distinguishable (Fig. 1E-H). Thus, the cause of death was renal failure due to the absence of a filtration apparatus. Heterozygote kidneys were indistinguishable from wild type in their morphological and histological features; hence we used 'wild type' throughout to encompass both genotypes, although the exact genotype is detailed in the figures.

To address the state of nephrogenesis, we used immunohistochemical methods to examine the residual renal tubules that were present in the mutant kidneys (green arrowheads in Fig.

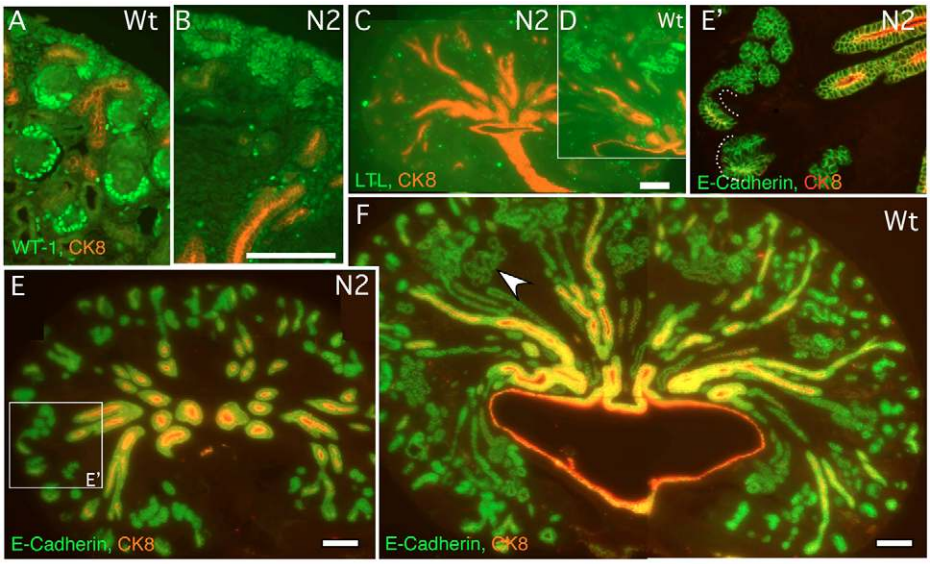

Fig. 2. Notch2-deficient kidneys (N2) develop distal tubules without formation of podocytes or proximal tubules. (**A**,**B**) Wild-type (A) kidney contains cells expressing high levels of Wt1 in glomerular podocytes and S-shaped bodies. The only cells that express low levels of Wt1 in the mutant (B) are mesenchymal cells surrounding cytokeratin-8-expressing ureteric buds (red). (**C**,**D**) LTL-stained proximal tubules found in wild type (D) are absent in the mutant (C). (**E**,**F**) Mutant kidney (E) develops numerous E-cadherin-positive, cytokeratin-8-negative distal tubules, some of which are connected to cytokeratin-8-positive ducts (dashed line in enlarged view E′). The wild-type proximal tubules, judged by morphology, also express E-cadherin (arrowhead in F). N2, Notch2 mutant; Wt, wild type. Scale bars: 0.1 mm in B for A,B,E′; in C for C,D.

1G,H and Fig. S2E in the supplementary material). Epithelial ductal labeling with anti-cytokeratin 8 (Ck8; Krt8 – Mouse Genome Informatics) antibodies (specific for UB derivatives) (Hemmi and Mori, 1991) confirmed that a branched collecting duct was present as expected (Fig. 2C,E). Expression of Wt1, a zinc-finger-containing transcription factor, expressed at low levels in the metanephric mesenchyme (MM) and at high levels in podocyte progenitors from the S-shaped body stage (Fig. 2A), was detected only in the MM surrounding the tips of the UB (Fig. 2B). Furthermore, whereas LTL, a marker specific for mature proximal convoluted tubules (PCT), labeled numerous tubules in wild type at E16.5 (Fig. 2D), no LTL-positive structures were detectable in the mutants (Fig. 2C). Thus, the organization of proximal fates was clearly compromised by Notch2 removal. By contrast, a comprehensive analysis of E-cadherin and Ck8 indicated that distal nephrons were Notch2-independent. Both RV-derived epithelia and collecting duct epithelium express E-cadherin, whereas Ck8 is expressed only in the collecting ducts. Many E-cadherin-positive, Ck8-negative tubular structures were detected in mutant kidneys. Several of these were continuous with the UB tips (Fig. 2E,E′). Whereas proximal tubules also express E-cadherin, the lack of LTL-binding activity, the continuity with the duct, their smaller size and the regular-shaped lumen (see Fig. 1H and see Fig. S2E in the supplementary material) indicate that renal tubules formed in the absence of Notch2 and most

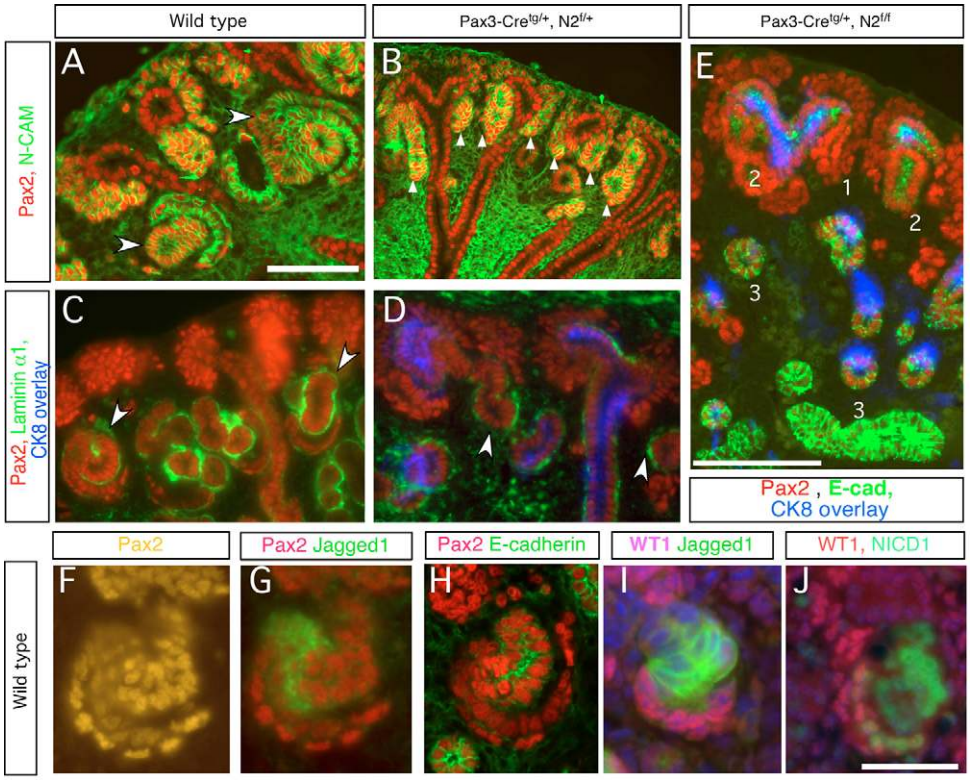

Fig. 3. Notch2-deficient mesenchyme undergoes normal epithelialization but the newly formed nephron fails to resolve into the S-shaped body seen in wild type. (**A-E**) Wild type (A) showing S-shaped bodies (arrowheads). In the Notch2 mutant, one nephron, expressing N-Cam, can be identified at each ureteric bud tip (arrowheads in B). These synthesize laminin α1 (arrowheads in D), as do the S-shaped bodies (arrowheads in C). (E) Three progressive stages during nephrogenesis in the mutant are marked as 1, 2 and 3. (**F-J**) Expression of molecular markers in each of the three segments in the S-shaped body (see text). Distal tubule precursors are Pax2^{High}- and E-cadherin-positive (F,H). Jag1 is localized in the middle segment in the position of proximal tubule precursors (G). Wt1 marks the podocyte precursors (I). N1-ICD is detectable in both the proximal and podocyte precursors (J). Scale bars: 0.05 mm in A for A-D and in J for F-J; 0.1 mm in E.

likely comprise only distal tubule segments of the nephron. Together, these data suggest that Notch2 is essential for the establishment of podocyte and PCT cell fates during nephron segmentation.

Notch2-deficient RVs initiate the segmentation process but fail to establish the proximal fates

To examine the early patterning of RV derivatives that preceded establishment of mature fates, we analyzed expression of a number of key reporters of these events. In both wild-type and mutant kidneys, a mesenchymal Pax2 domain forms around the UB tip (Fig. 3A,B and data not shown). $Pax2^{High}$ mesenchymal cells were congregated around the tips of the UB (compare with Wt1 staining in Fig. 2B). Neural cell adhesion molecule (N-Cam; Ncam1 – Mouse Genome Informatics) is expressed in the mesenchymal cells and in their derivatives, including the nascent renal vesicle. In wild type, N-Cam-positive cell clusters with elevated Pax2 expression appeared adjacent to the UB tip (Fig. 3A). In Notch2 mutants, we detected similar groups of amorphic $Pax2^{High}$, N-Cam-positive, Ck8-negative structures located close to the UB tips (Fig. 3B,E). These clusters were positive for two signature processes of epithelialization: cellular polarization, indicated by formation of a laminin α1-positive basal lamina deposition (Abrahamson et al., 1989) (Fig. 3C,D), and the synthesis of epithelial adhesion molecules (E-cadherin, Fig. 3E). Therefore, a robust mesenchymal condensation and mesenchymal-epithelial transition occurs normally in Notch2-deficient metanephric mesenchyme.

The analysis of E-cadherin expression revealed three types of epithelial structures in the Notch2 mutant kidneys. First, the aforementioned early RVs: small cell clusters located just below the tips of the UB that expressed $Pax2^{High}$ (#1 in Fig. 3E); the second, larger epithelial clusters of Pax2 positive, E-cadherin-positive cells (#2 in Fig. 3E), a structure potentially analogous to comma- or S-shaped bodies or a 'transitional' structure between the early RV and S-shaped body; and a third structure that was tubular in shape, $Pax2^{Low}$ and E-cadherin-positive (#3 in Fig. 3E).

We examined the expression of Wt1, cadherin 6 and E-cadherin for any evidence of putative podocyte or proximal tubule precursors in the Notch2-deficient renal epithelia. As was the case with LTL, cadherin 6, an adhesion molecule thought to be expressed in the precursors of PCTs in S-shaped bodies, was not detected in Notch2-deficient kidneys (Fig. 4A,B). Further, $Wt1^{High}$ podocyte precursors were also absent (Fig. 4A′,B′). On close examination, the data suggested that proximal segmentation initiated, but failed to establish independent proximal identities. During early stages of nephrogenesis preceding formation of the S-shaped body, Pax2 is expressed in all epithelia and is required to initiate expression of Wt1 (Dehbi et al., 1996); upregulation of Wt1 inhibits Pax2 expression (Dehbi et al., 1996; Ryan et al., 1995). As in the wild type (Fig. 4A′,A″), we observed Wt1 expression in Notch2-deficient nephrons that appeared to segregate from Pax2, such that cells containing lower levels of Wt1 displayed relatively higher levels of Pax2 and vice versa (Fig. 4B′,B″;4A‴,B‴). Further evidence of polarity comes from analysis of Lim1 (Lhx1 – Mouse Genome Informatics); Lim1 expression is restricted to cells within the RV that are closest to the UB tip (Fig. 4C), and this is observed in Notch2 mutant kidney (Fig. 4D). Thus, the initiation of RV polarity appears to be Notch2-independent, but the establishment of stable regional identities in distinct proximal and distal regions of the developing nephron is defective and proximal fates are absent from the S-shaped body.

To address Notch pathway activation in normal nephron segmentation, we analyzed the spatial and temporal expression domain of Notch pathway proteins, in conjunction with segment-specific markers. Jag1 protein was first detected in clusters of $Pax2^{Low}$-expressing epithelial cells in early RVs (Fig. 4E). In the absence of a good antibody to Dll1, we monitored the presence of LacZ knocked into the *Dll-1* gene in *Dll-1*^{LacZ} heterozygotes (Hrabe de Angelis et al., 1997). *Dll-1*^{LacZ} was also present in a subset of RV cells (Fig. 4G) that also contained activated Notch1 (Fig. 4H,I) and Lim1 (Fig. 4C). Jag1 expression and N1-ICD accumulation became

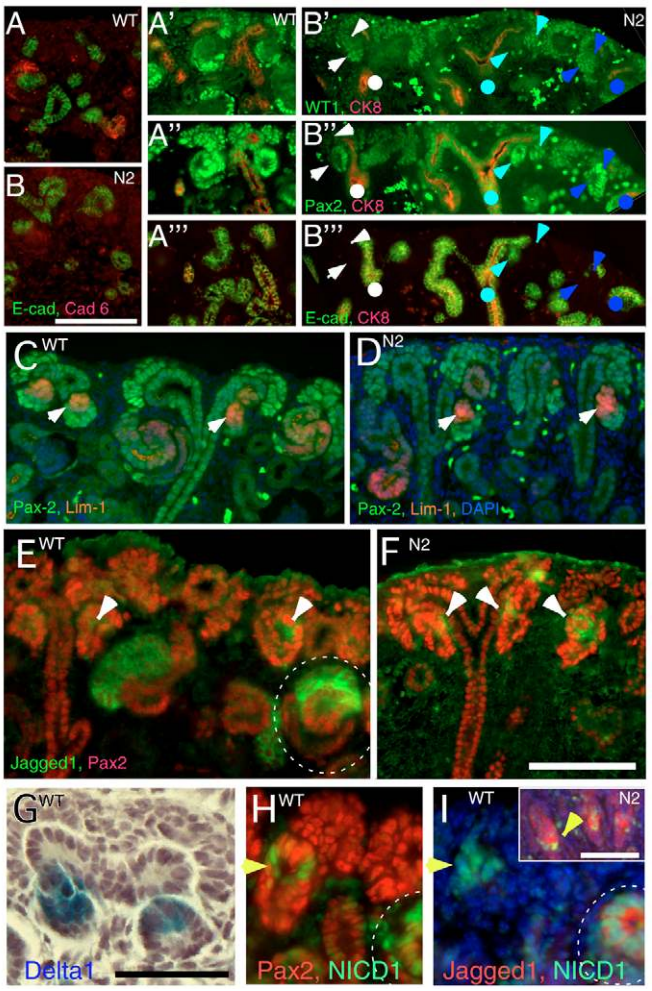

Fig. 4. The segmentation process in Notch2-deficient nephron (N2) is impaired. (**A**,**B**) Cadherin-6-expressing cells are adjacent to E-cadherin-expressing cells in wild type (A), but no cadherin-6-expressing cells are detectable in mutant (B). (**A′-B‴**) Serial sections stained with the segmentation markers Wt1, Pax2 and E-cadherin. Circles and arrowheads locate the same cells in adjacent sections to indicate similar structure across all sections. (**C**,**D**) Lim1 expression pattern in the renal vesicle is similar in wild-type and Notch2 mutant kidneys (white arrows). The cells at the very proximal end of the mutant nephron express high levels of Lim1 (D). This distribution is different from that in a wild-type S-shaped body (C). (**E**) In wild type, few Jag1-expressing cells are seen in the renal vesicle (arrowheads), but the population expands with the formation of the S-shaped body (circle). (**F**) A small cluster of Jag1-expressing cells is seen in each of the mutant nephrons. (**G**,**H**) *Dll-1*^{LacZ} and N1-ICD (arrowhead) are detectable in the renal vesicle in wild type. (**I**) In some cases, Jag1 is not co-localized with N1-ICD (arrowhead). N1-ICD remains detectable in Notch2-deficient nephrons (arrowhead, inset in I). Scale bars: 0.1 mm in B for A-B‴ and in F for C-F; 0.05 mm in G-I.

elevated on morphogenesis of the RV to the S-shaped body (Fig. 3G,I,J, Fig. 4C,G). Although the cell fates have not been mapped to date, these observations suggest that activated Notch1, Jag1 and Dll-1^{LacZ} expression are likely to mark more proximal precursor populations within RVs and their early derivatives and are thus among the first markers of segmentation. Distal precursors within the S-shaped body expressed E-cadherin and high levels of Pax2 (Pax2^{High}) (Ryan et al., 1995), but no Jag1 or N1-ICD (Fig. 3F,H,I). Podocyte precursors were Wt1-positive, Pax2^{Low}- and Jag1-negative; some contained N1-ICD (Fig. 3J, Fig. 4F,I; see Fig. S3C in the supplementary material). In the S-shaped body, *Dll-1^{LacZ}* expression overlapped with, but was broader than, the *jag1* domain in most S-shaped bodies. Whether this reflects real differences or the possible perdurance of β-galactosidase activity is unclear. Dll1^{LacZ} was detected in a few E-cadherin-expressing distal precursors and in some podocyte precursors (see Fig. S4D in the supplementary material). In this respect, the *Dll-1^{LacZ}* expression domain resembled the pattern of Notch1 activation better than the Jag1 domain (see Fig. S4C,D in the supplementary material). We suggest that Jag1-positive, *Dll-1^{LacZ}*-expressing, N1-ICD-containing, Pax2^{Low} cells probably define proximal regional fates, and Jag1 is likely to be a better marker of PCT precursors than *Dll-1* (the functional significance of *Dll-1* is discussed below). Unfortunately, while a detailed in situ expression analysis has been published for Notch receptors (Chen and Al-Awqati, 2005; Leimeister et al., 2003; Piscione et al., 2004), the absence of a suitable antibody has prevented mapping of Notch2 protein distribution.

We next addressed whether the Jag1-expressing proximal region precursors within the RV and early RV derivatives, the first to downregulate Pax2 (Fig. 3F,G), contain N1-ICD in Notch2-deficient kidneys. A small group of Jag1-expressing cells were detected in virtually every Notch2-deficient early epithelial clusters (Fig. 4F,I), consistent with the possibility that initiation of proximal patterning is initially independent of Notch2. N1-ICD was detectable in these Jag1-expressing cells (Fig. 4I inset), indicating that Notch1 signaling was apparently active in these cells. Clearly, Notch1 activity could not compensate for the loss of Notch2 in subsequent patterning steps. This observation leaves open the possibility that Notch1 may contribute to the establishment of the earliest polarity pathway. Note that Pax2 expression in Jag1-positive, Notch2-deficient cell clusters in the RV derivatives remained ubiquitous and high, consistent with impairment in acquisition of proximal and podocyte fates.

In conclusion, segregation of Wt1, Pax2 and Lim1 expression initiated and was accompanied by transient acquisition of a proximal precursor fate (Jag1-positive, N1-ICD present). However, podocyte precursors (Wt1^{High}) never formed. This is because Notch2-deficient epithelial cells could not resolve proximal from distal fates, as evident from the simultaneous expression of markers typical for proximal and distal differentiation at the S-shaped stage. Notch2-deficient cells either die or adopt a Notch2-independent distal fate. We thus conclude that the transitional epithelial structures marked as #2 in Fig. 3E represent defective comma- or S-shaped bodies in which segmentation has initiated but the specification of appropriate regional identities has failed.

Notch2-deficient proximal precursors have reduced capacity to proliferate

Three hypotheses can explain why morphologically distinct comma- and S-shaped bodies fail to form in the Notch2-deficient kidneys. First, cells with dual identity (i.e. expressing both Jag1 and Pax2) die, resulting in failure to form comma- and S-shaped bodies. Second, due to global proliferation defects in the early renal epithelia, abnormal epithelial structure forms. Third, Jag1-positive proximal tubule precursors are unable to expand, and, in their absence, typical S-shaped bodies fail to form.

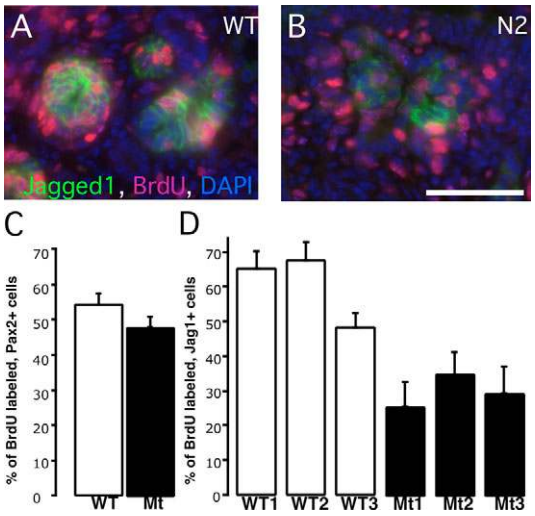

Fig. 5. Notch2 mutant, Pax2-expressing early renal epithelia proliferate as wild-type, whereas Jag1-expressing, Notch2-deficient clusters have few cycling cells. (**A**,**B**) Representative images of BrdU incorporation (red) within the Jag1-expressing clusters (green) in wild type and mutant. (**C**,**D**) Histograms of results from several embryos indicate the percentage of BrdU-labeled cells within the Pax2- or Jag1-expressing domains. Data are presented as means±s.e.m. Scale bar: 0.05 mm.

The first possibility was addressed by examining the distribution of active caspase3, an early marker of apoptosis; no significantly enhanced apoptosis was observed (data not shown). The second explanation was addressed by pulse-labeling S-phase cells with BrdU and the fraction of Pax2^{High} cell examined in renal epithelia close to the UB tips; we observed a BrdU-positive fraction of ~50% in both wild-type and *Notch2* mutant metanephroi (54 versus 48%, $P>0.1$; Fig. 5). Thus, a general proliferative defect does not underlie abnormal tubule morphogenesis in Notch2 mutants. When proliferation was scored specifically in Jag1-expressing cells, the subpopulation of *Notch2*-deficient, Pax2^{High}, *Jag1*-expressing cells entered the cell cycle twofold less frequently than their wild-type counterparts ($F_{(6, 15)}=8.697$, $P<0.001$; Fig. 5). Therefore, Notch2 activity is required for normal proliferation of proximal regional precursors.

Notch1 is not required for cell fate determination during early nephron formation

To test if Notch2 was sufficient on its own for nephron segmentation in the absence of any Notch1 input, we generated *Pax3-cre$^{tg/+}$; N1$^{f/f}$* embryos. However, these failed to survive beyond E9.5 (data not shown) and consequently were uninformative. Two alternative strategies were adopted. First, we used chimera analysis with ES cells deficient for Notch1 (Fig. 6). Second, we used *Pax2-cre* transgenic mice (Fig. 7) (Ohyama and Groves, 2004).

We examined chimeric kidneys generated by injecting *N1$^{Δ1/Δ1}$; Rosa26-lacZ$^{tg/+}$* ES cells (see Hadland et al., 2004; Nichols et al., 2004) into wild-type blastocysts. N1^{Δ1} contains a large deletion of the locus (Conlon et al., 1995). We analyzed seven chimeric

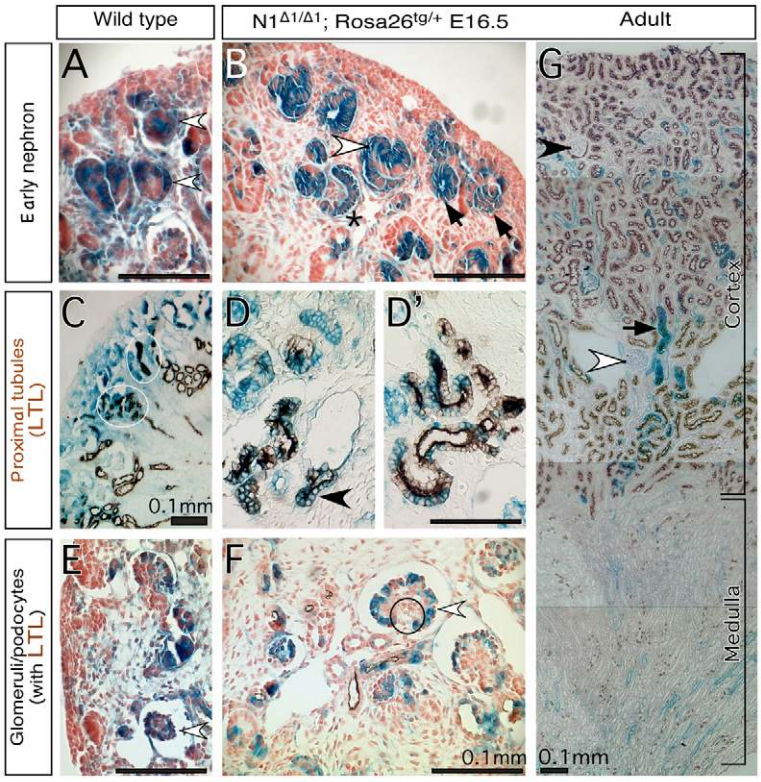

Fig. 6. Notch1-deficient ES cells contribute to various parts of the nephron. Kidneys were harvested from E16.5 embryos (**A-F**) or adults (**G**) and subjected to whole mount β-gal staining. (A,C,E) Wild-type ES cells in E16.5 kidneys are found in early nephrons (arrowheads in A), PCTs (circled in C) and glomerular podocytes (arrowhead in E). (B,D,F,G) *Notch1*$^{-/-}$*; Rosa26* ES cells contribute to renal vesicles (arrows in B), S-shaped bodies (arrowhead in B) and podocytes in the capillary-loop stage (star in B). (D,D′) Notch1-deficient ES cells (blue) contribute to LTL-labeled PCT together with wild-type cells (unstained). One LTL-labeled cross-section composed entirely from Notch1-deficient cells is shown in D (arrowhead). (F) Glomerular podocytes develop in the absence of Notch1 (arrowhead). The circle indicates the capillary lumen with red blood cells in it. (G) The adult chimeric kidney is stained with LTL (brown). Some of the LTL-labeled tubules in the inner cortex are entirely derived from Notch1$^{-/-}$ cells (black arrow). White and black arrowheads indicate a juxtamedullary glomerulus and a cortical glomerulus, respectively.

mice with *Rosa26*$^{tg/+}$, *N1*$^{\Delta 1/\Delta 1}$ cells and four with matched *Rosa26*$^{tg/+}$ wild-type controls. In all, lacZ-positive cells contributed extensively to normal-looking RVs, S-shaped bodies and elongating nephrons, consistent with the absence of an early function for Notch1 (Fig. 6B). Many glomeruli were composed entirely from *Notch1*-deficient podocytes. The number of N1$^{\Delta 1}$ podocytes that surrounded a wild-type capillary tuft were within the normal range (Fig. 6F). Further, the contribution of the *Notch1*-deficient cells to the LTL^{+} proximal convoluted tubules was also extensive (Fig. 6D,D′). Thus, there is no cell-autonomous requirement for Notch1 activity to establish proximal renal tubule fates; however, we could not rule out a non-autonomous contribution from Notch1-expressing cells intermingled with N1$^{-/-}$ cells.

To determine whether any requirement for Notch1 exists, a *Pax2-cre*^{tg} transgene was used to remove Notch1 function from the metanephric kidney. Cre-mediated recombination is catalyzed in the condensing metanephric mesenchyme and in UB derivatives (see Fig. S3A-B in the supplementary material) (Ohyama and Groves, 2004). Compound heterozygote *Pax2-cre*^{tg}; *N1*$^{f/\Delta 1}$ embryos were normal at E12.5 but died at E13.5 from unrelated vascular failure and hemorrhage in the internal organs (data not shown). We therefore removed the E12.5 metanephroi from *Pax2-cre*$^{tg/+}$*; N1*$^{f/\Delta 1}$ embryos and littermate controls (some of which also carried the *Dll1*^{lacZ} allele) and examined their development.

Notch1 protein is detected in the plasma membranes of duct and renal epithelial cells (inset in Fig. 7C; see Fig. S3E-F in the supplementary material). Intense apical staining indicates accumulation of Notch1 in S-shaped bodies (inset in Fig. 7C; see Fig. S3E-F in the supplementary material). Staining for Notch1 protein confirmed it was absent in duct and renal epithelia of *Pax2-cre* containing metanephroi (inset in Fig. 7D; see Fig. S3G-L in the supplementary material). Accordingly, no accumulation of N1-ICD was detected in renal epithelia of *Pax2-cre*$^{tg/+}$*; N1*$^{f/\Delta 1}$ embryos (see Fig. S3C-D in the supplementary material). By contrast to Notch2, Notch1-deficient metanephroi appeared morphologically and histologically normal; they contained LTL-positive proximal tubules (Fig. 7B), E-cadherin-positive and Ck8-negative distal tubules (not shown) and Wt1^{High}, synaptopodin-positive (Mundel et al., 1997) podocytes (Fig. 6D). By contrast, *Pax2-cre*$^{tg/+}$*; N2*$^{f/f}$ embryos developed kidneys lacking proximal tubule and podocytes (data not shown), indicating that *Pax2-cre*$^{tg/+}$ used in this study removes Notch alleles before the critical window described previously (Cheng et al., 2003). Thus, Notch1 is not required for regional organization of distinct cell fates.

Rbp-J deletion mimics the effect of Notch2 deficiency on nephron formation

One possible explanation for the crucial role of Notch2 and the failure of active Notch1 signaling to normally complement Notch2 action would be that Notch2 has acquired a unique, Rbp-J-independent activity. To address this issue, we generated *Pax2-cre*$^{tg/+}$*; Rbp-J*$^{f/f}$ mice (Tanigaki et al., 2002). *Pax2-Cre*$^{tg/+}$*;Rbp-J*$^{f/f}$ embryos were normal at E12.5 but died at E13.5; when cultured at E12.5, metanephroi from *Pax2-cre*$^{tg/+}$*; Rbp-J*$^{f/f}$ embryos branched properly but failed to produce LTL-positive proximal convoluted tubules or Wt1^{High} podocytes (Fig. 7E-H). Thus, it appears that Notch2 acts in a conventional, Rbp-J-dependent pathway during nephron segmentation.

Notch1 can stimulate proximal fates and inhibit distal ones when ectopically activated in nephron precursors

A second possible explanation for the failure of Notch1 signaling to compensate for Notch2 could be a requirement for distinct levels of signaling inputs; the existence of activation thresholds for the Notch

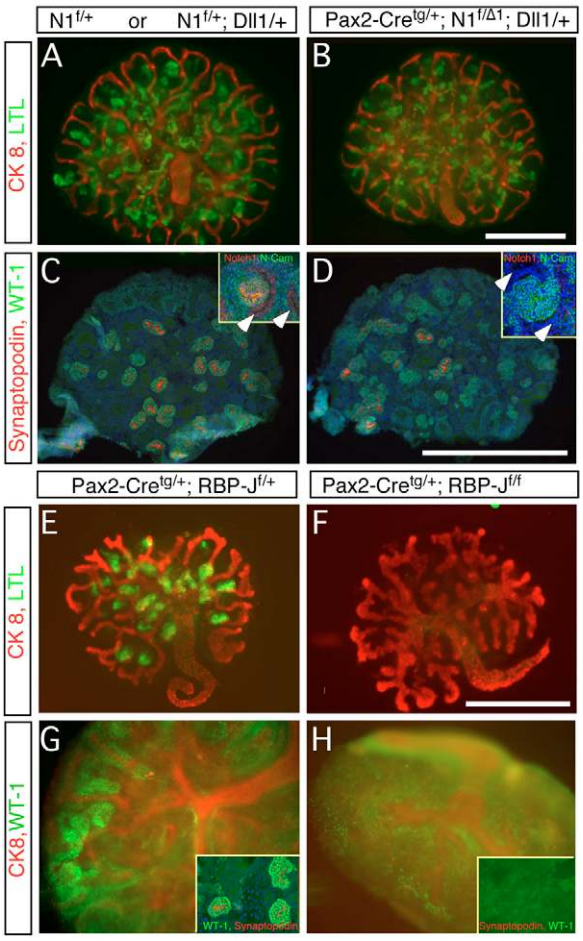

Fig. 7. Notch1-deficient metanephroi are phenotypically wild type. Genotypes are marked above all panels. Where indicated, floxed alleles were recombined with the Pax2-Cre$^{tg/+}$ strain. (**A**,**B**,**E**,**F**) Whole-mount staining of LTL (green) and Ck8 (red) detects extensive renal tubulogenesis. Loss of Notch1 did not alter proximal tubule formation (B), whereas loss of Rbp-J resulted in loss of LTL-positive epithelial cells (F). Note that loss of Notch1 (see Notch1 staining in inset in C,D) or of Rbp-J in the duct did not prevent duct branching. (**C**,**D**,**G**,**H**) Glomerular podocytes are labeled with Wt1 (green). In G,H, whole-mount preparation is also stained with Ck8 (red). Wt1^{High}, synaptopodin-positive (red in C,D, inset in G) glomeruli are present in wild type (C), Notch1-deficient metanephroi (D) and Rbp-J heterozygotes (G), but not in Rbp-J deficient metanephroi (inset in H, no Wt1 or synaptopodin). Scale bars: 0.5 mm in B for A,B; in D for C,D; in F for E-F.

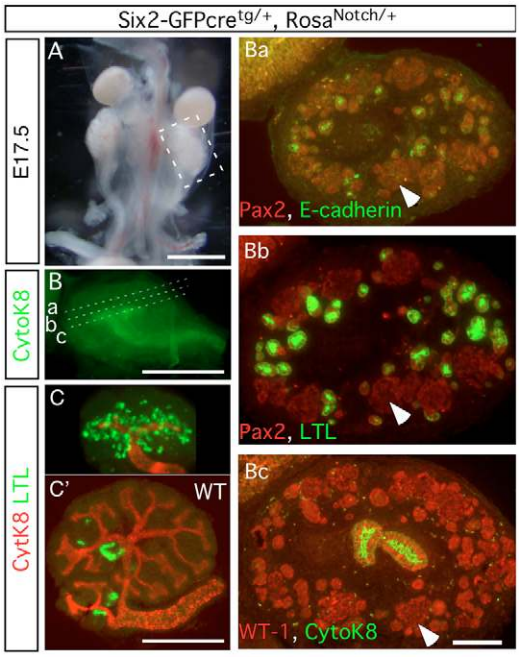

Fig. 8. Constitutively active Notch1 promotes proximal tubule formation while inhibiting the progenitor from differentiating into podocytes and distal tubules. (**A**) Notch1 activation in the mesenchyme causes renal hypoplasia at E17.5. (**B**) The ureteric bud branches only once. Subsequent planes of sectioning are marked (a-c). Ck8 is visualized using Cy3, but the image is pseudocolored to correspond with Ba-Bc. (**C**,**C′**) E11.5 metanephroi from mutant (C) or wild type (C′) were cultured for 4 days, stained with LTL (green) and Ck8 (red). (Ba-Bc) Serial sections of the mutant kidney stained with markers for renal tubules. Arrowheads locate the same cells in adjacent sections. Scale bars: A,B,C,C′, 0.5 mm; Ba-Bc, 0.1 mm.

targets Hes1 and Hes5 was recently demonstrated in organ culture (Ong et al., 2006). If so, higher amounts of N1-ICD may be able to compensate for Notch2 in activating its targets and promoting formation of proximal pattern.

To test this hypothesis, we used a metanephric mesenchyme-specific line *Six2-GFP::Cre*. This Cre strain will be described more fully elsewhere. Importantly, *Six2-GFP::Cre* is active in the cap stage, slightly later than the *Pax2-cre* but before RV formation (Xu et al., 2003). Hence, a stable recombination results in a genetic modification of the MM and its derivatives. To elevate N1-ICD levels, we created *Rosa^{Notch}/+; Six2-GFP::Cre$^{tg/+}$* mice. In these animals *Six2-GFP::Cre* excises a 'stop' cassette and constitutive expression of N1-ICD activates Notch1 signaling (Murtaugh et al., 2003). Pups with this genotype were born in the correct Mendelian ratio but displayed severely hypoplastic kidneys (Fig. 8A) in which the UB underwent a single branching event (Fig. 8B). The absence of Six2-producing cells at E13.5 in the *Rosa^{Notch}/+; Six2-GFP::Cre$^{tg/+}$* kidney suggested that lack of branching was secondary to the loss of glial cell line-derived neurotrophic factor-producing MM cells (data not shown).

Despite the branching deficit, multiple tubular epithelial structures formed from the Wt1; Pax2 positive cell clusters (Fig. 8Ba-c). These tubular epithelia expressed both LTL (Fig. 8Bb,8C) and Slc34a1 (not shown), characteristic of PCTs. To determine whether activated Notch1 accelerated the formation of proximal tubules, E11.5 metanephroi were cultured for 4 days. At this stage, there were very few LTL-positive tubules present in wild type; however, metanephroi that overexpressed N1-ICD had already developed numerous LTL-positive tubules (Fig. 8C,C′). Furthermore, the activity of N1-ICD was independent of Notch2, as LTL-positive PCTs appeared even in the presence of DAPT (Fig. 9). In summary, N1-ICD can direct development of proximal nephron fates that are normally controlled by Notch2, consistent with a model in which N1-ICD is present at subthreshold levels during normal nephron patterning.

DISCUSSION

Notch2 maintains or induces proximal fates in the developing nephron

Mesenchymal cells in the metanephric blastema form renal epithelia in response to factors secreted by the UB tips (Carroll et al., 2005). The first epithelial structure (early RV stage) lacks distinctive

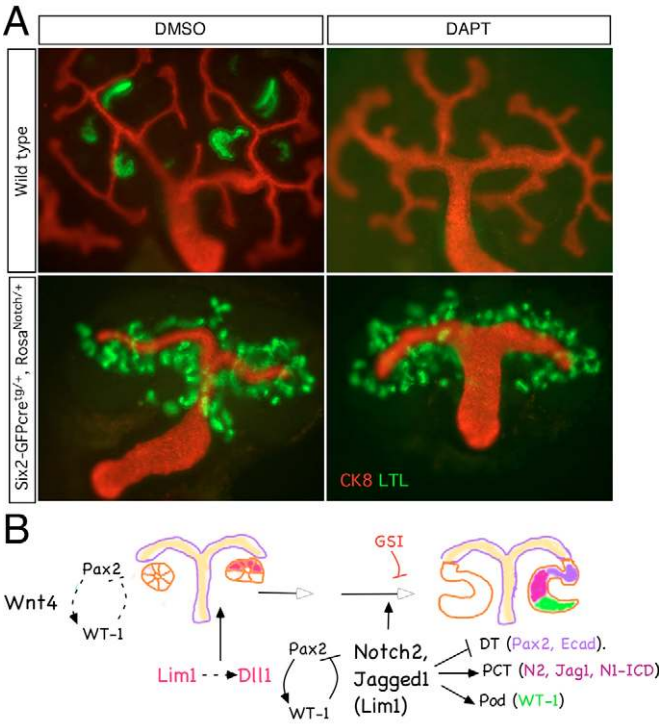

Fig. 9. N1-ICD directs PCT fates independent of Notch2. (**A**) Ectopic overexpression of Notch1 intracellular domain is sufficient to promote proximal tubule formation in the absence of γ-secretase activity. Genotypes are shown to the left of the image. DMSO, vehicle only; DAPT, γ-secretase inhibitor. (**B**) Schematic of the proximalization pathway. After RV induction (a Wnt-dependent process), Pax2 and Wt1 begin to separate into distinct expression domains and Lim1 and Dll1 define a distal domain within the RV. However, Notch2 signals are required for separation of proximal from distal fates; in their absence (or when blocked by γ-secretase inhibitors), only distal tubules form. See text for details. GSI, γ-secretase inhibitors.

morphological features, although the expression patterns of genes such as *Brn-1* (Nakai et al., 2003) suggest that polarization starts soon after epithelialization. Within the asymmetrical comma- and S-shaped body, molecular markers of the three main epithelial lineages (distal tubules, proximal tubules and podocytes) map to discrete epithelial domains. This process of renal epithelial segmentation may still require 'classical', UB-derived inductive function as mesenchyme induced for a shorter time only gives rise to distal tubule fates, whereas the formation of morphologically distinct proximal tubules and podocytes from MM requires at least 24 hours exposure to the inducer (Saxen, 1987). Moreover, the ability of Pax2 to induce Wt1, and the ability of Wt1 to inhibit Pax2 (Ryan et al., 1995), should be enough to support segregation of the podocyte lineage from the distal tubule, but is not sufficient to account for formation of PCTs.

Recently, it was demonstrated that segmentation required γ-secretase activity (Cheng et al., 2003; Wang et al., 2003), an enzyme with many substrates, including Notch receptors (Kopan and Ilagan, 2004). Moreover, the sensitivity of renal epithelia to γ-secretase inhibitors is informative: distal tubules are resistant to the drug, whereas proximal tubules and podocyte are sensitive to it. Once S-shaped bodies form, they are no longer sensitive to the inhibitor (Cheng et al., 2003). This observation suggested that a γ-secretase-dependent process acts to establish podocyte and proximal tubule identities in RV derivatives. In this report, we identify Notch2 as the first key determinant involved in acquisition of proximal fates in the nephron.

The idea that Notch signaling may provide this function is supported by marker analysis. Until recently, only a few markers had distinguished the segments within the S-shaped body: Wt1 marks podocyte precursors (Kreidberg et al., 1993), cadherin 6 probable proximal tubule precursors, and E-cadherin and Brn-1 more distal tubule precursors (Cho et al., 1998; Nakai et al., 2003). The usefulness of Pax2 as a segmentation marker has been underappreciated; differential expression distinguishes prospective distal and Bowman's capsule precursors from proximal precursors and podocytes (this study) (Ryan et al., 1995). Examination of all these markers, Notch ligands and Notch1 activation suggests that segmentation initiates within the RV or its earliest derivative. Here, a small subset of cells acquires proximal precursor markers (Jag1, activated Notch1); expression may be activated at the boundary of Lim1-positive and -negative territories. N1-ICD and Jag1 may provide the earliest markers for proximal tubule precursors; we anticipate that this population expands and expresses cadherin 6, and develops into mature proximal tubules that are LTL^{+}.

Our studies indicate that activated N1-ICD, Lim1 and Jag1 are all observed in the RV of Notch2-deficient newborn mice; thus, it is likely that segmentation initiates independently of Notch2. However, persistent expression of the distal tubule marker (Pax2^{High}) suggests a function for Notch in Pax2 inhibition, while the reduced proliferation rates of Jag1-expressing cells suggest Notch2 promotes the proliferative expansion of this progenitor domain. Asymmetrical expression of *Dll-1*^{LacZ} in the RV is another early indicator of RV segmentation (Fig. 4G). Kobayashi et al. (Kobayashi et al., 2005) have shown that Lim1-deficient kidneys produce lower *Dll-1* and arrest at the RV stage. Part of the Lim1 phenotype may be explained by failure to activate *Dll-1* and hence Notch2 at this stage. Indeed, hypomorphic *Dll-1* allele (Kiernan et al., 2005) results in reduction of proximal tubule formation (see Fig. S4 in the supplementary material). These observations suggest that Lim1 can serve as an upstream regulator of Notch ligands, and thus Notch signaling. However, Lim1$^{-/-}$ ES cells do not contribute to the regions of the comma- and S-shaped bodies, indicating that Dll1-expressing, wild-type cells cannot rescue Lim1-deficient cells. Lim1 is thus required also during proximalization. The early RV distribution of Lim1 was maintained in the Notch2-deficient RV (Fig. 4D), but in the more advanced nephron Lim1 expression assumed an abnormal pattern: although they will all eventually adopt the distal fate, cells accumulating at the proximal end expressed high Lim1 (Fig. 4C). Therefore, the separation of the distal and proximal lineages and the differentiation of proximal tubule and podocyte precursors require two parallel inputs, one provided by Notch2 and another from Lim1.

Notch1 and Notch2 have non-overlapping activities

We demonstrate here that while direct activation of Notch1 is observed in proximal precursors of the S-shaped body, removal of Notch1 activity with *Pax2-Cre* had no impact on the establishment of proximal fates. Thus, Notch1 is clearly non-essential for this process and Notch2 is the only γ-secretase substrate that plays a significant role in these patterning events. As soon as Notch was identified as an X-linked locus in *Drosophila* (Welshons, 1958), it was realized that the wing phenotype associated with Notch mutations was due to haploinsufficiency. Notch1 is haploinsufficient in vertebrates as well: myelination in the mouse is slowed in Notch1 heterozygote animals (Givogri et al., 2002), and human tricuspid

heart valve development and maintenance of valve flexibility throughout adult life require both alleles of Notch1 (Garg et al., 2005). Importantly, no kidney disease is reported in these kindred; however, as this manuscript underwent revisions, a human haploinsufficiency for Notch2 was reported to cause Alagille syndrome (McDaniell et al., 2006). This would not be possible if Notch1 and Notch2 played redundant roles in human nephron development; we infer from this data that in human, as in the mouse, Notch2 is the dominant receptor during nephron segmentation.

While Notch1 and Notch2 differ in their ability to activate targets (Ong et al., 2006), they have the same affinity to Rbp-J (Lubman et al., 2006). Notch-responsive promoters may respond differentially to similar nuclear concentrations of activated Notch receptors within the nephron, becoming inactive if this amount falls below a threshold (Ong et al., 2006). What then can be the mechanistic basis for these findings?

The observation that N1-ICD overexpression can promote the proximal fates when endogenous Notch processing (and thus signaling) is abolished supports a model whereby subthreshold levels of this protein in the normal renal epithelium fail to complement Notch2 deficiency. Thus, Notch1 may be a weak activator of key target(s) regulated normally by Notch2, or N1-ICD may fail to accumulate to sufficient levels in the normal kidney to functionally replace Notch2 deficiency. Another possibility is that N1-ICD is modified in a manner that decreases its odds of association with Rbp-J. This will be predicted to prevent its degradation (Fryer et al., 2004), and ironically, facilitate its detection by immunohistochemistry. When overexpressed, some N1-ICD may escape modification, bind and activate crucial targets.

If differences existed between N1-ICD and N2-ICD that affected binding to Rbp-J or to other putative partners, where would they map within the intracellular domain? Domain swaps indicated that the divergent 426 amino acids that lie downstream of the ANK domain are not important: mice expressing a Notch2 hybrid containing this Notch1 domain (and thus deficient in the Notch2 C-terminal domain) lack a kidney phenotype (Kraman and McCright, 2005). Crystallographic analysis of the Notch1 ANK domain revealed a surface unique to each of the vertebrate Notch paralogs (Lubman et al., 2005). Therefore, the subtle differences in the ANK domain may be responsible for the lack of redundancy between these highly conserved receptors (see also Ong et al., 2006).

In conclusion, our study presents the first evidence for the crucial role of Notch2 in an intrinsic patterning mechanism that establishes proximodistal nephron polarity. We discovered a cell type in which two different Notch molecules are present in its nucleus yet only one is crucial (Notch2), a demonstration of unexpected complexity in this pathway, and provided evidence that detection of N1-ICD per se is not an unambiguous indicator of a functional role for Notch1 signaling. These results serve as an entry point to explore further details of the mechanisms controlling early nephron development. They establish that Notch2 acts to separate proximal and distal fates, and in this Notch signaling most likely plays an instructive role after an initial polarizing cue (Lim1?) acts in the RV. Thus, utilization of Notch proteins in the kidney appears to be quite different from their use in the skin, where all cellular identities emerge before, and independent of, Notch function (Pan et al., 2004) and where Notch1 plays a dominant role (S. Demehri, Y. Pan and R.K., unpublished).

The authors wish to thank Dr Jeff Miner for careful reading of the manuscript and numerous consultations throughout the course of this work, and Drs Andrew Groves (for the Pax2-cre mice) and Jonathan Epstein (for the Pax3-cre mice), Thomas Gridley (for the conditional Notch2 mice) and Tasuku Honjo (for the conditional Rbp-J mice). R.K., H.-T.C., M.K. and K.S. were supported by a grant from the NIH-NIDDK (DK066408); M. Kim was also supported by the Korea Research Foundation Grant (KRF-2004-214-C00106). Work in APM's laboratory was supported by a grant from the NIH-NIDDK (DK054364). MTV received support from an NRSA granted by NIH-NIDDK (5F32DK060319).

Supplementary material

Supplementary material for this article is available at http://dev.biologists.org/cgi/content/full/134/4/801/DC1

References

Abrahamson, D. R., Irwin, M. H., St John, P. L., Perry, E. W., Accavitti, M. A., Heck, L. W. and Couchman, J. R. (1989). Selective immunoreactivities of kidney basement membranes to monoclonal antibodies against laminin: localization of the end of the long arm and the short arms to discrete microdomains. *J. Cell Biol.* **109**, 3477-3491.

Carroll, T. J., Park, J. S., Hayashi, S., Majumdar, A. and McMahon, A. P. (2005). Wnt9b plays a central role in the regulation of mesenchymal to epithelial transitions underlying organogenesis of the mammalian urogenital system. *Dev. Cell* **9**, 283-292.

Chen, L. and Al-Awqati, Q. (2005). Segmental expression of Notch and Hairy genes in nephrogenesis. *Am. J. Physiol. Renal Physiol.* **288**, F939-F952.

Cheng, H., Miner, J., Lin, M., Tansey, M. G., Roth, K. A. and Kopan, R. (2003). g-secretase activity is dispensable for the mesenchyme-to-epithelium transition but required for proximal tubule formation in developing mouse kidney. *Development* **130**, 5031-5041.

Cho, E. A., Patterson, L. T., Brookhiser, W. T., Mah, S., Kintner, C. and Dressler, G. R. (1998). Differential expression and function of cadherin-6 during renal epithelium development. *Development* **125**, 803-812.

Conlon, R. A., Reaume, A. G. and Rossant, J. (1995). Notch1 is required for the coordinate segmentation of somites. *Development* **121**, 1533-1545.

Dehbi, M., Ghahremani, M., Lechner, M., Dressler, G. and Pelletier, J. (1996). The paired-box transcription factor, PAX2, positively modulates expression of the Wilms' tumor suppressor gene (WT1). *Oncogene* **13**, 447-453.

Engleka, K. A., Gitler, A. D., Zhang, M., Zhou, D. D., High, F. A. and Epstein, J. A. (2005). Insertion of Cre into the Pax3 locus creates a new allele of Splotch and identifies unexpected Pax3 derivatives. *Dev. Biol.* **280**, 396-406.

Fryer, C. J., White, J. B. and Jones, K. A. (2004). Mastermind recruits CycC:CDK8 to phosphorylate the Notch ICD and coordinate activation with turnover. *Mol. Cell* **16**, 509-520.

Garg, V., Muth, A. N., Ransom, J. F., Schluterman, M. K., Barnes, R., King, I. N., Grossfeld, P. D. and Srivastava, D. (2005). Mutations in NOTCH1 cause aortic valve disease. *Nature* **21**, 180-184.

Givogri, M. I., Costa, R. M., Schonmann, V., Silva, A. J., Campagnoni, A. T. and Bongarzone, E. R. (2002). Central nervous system myelination in mice with deficient expression of Notch1 receptor. *J. Neurosci. Res.* **67**, 309-320.

Grieshammer, U., Cebrian, C., Ilagan, R., Meyers, E., Herzlinger, D. and Martin, G. R. (2005). FGF8 is required for cell survival at distinct stages of nephrogenesis and for regulation of gene expression in nascent nephrons. *Development* **132**, 3847-3857.

Hadland, B. K., Huppert, S. S., Kanungo, J., Xue, Y., Jiang, R., Gridley, T., Conlon, R. A., Cheng, A. M., Kopan, R. and Longmore, G. D. (2004). A requirement for Notch1 distinguishes two phases of definitive hematopoiesis during development. *Blood* **104**, 3097-3105.

Hemmi, A. and Mori, Y. (1991). Immunohistochemical study of cytokeratin distribution in the collecting duct of the human kidney. *Acta Pathol. Jpn.* **41**, 516-520.

Hrabe de Angelis, M., McIntyre, J., 2nd and Gossler, A. (1997). Maintenance of somite borders in mice requires the Delta homologue Dll1. *Nature* **386**, 717-721.

Karavanov, A. A., Saint-Jeannet, J. P., Karavanova, I., Taira, M. and Dawid, I. B. (1996). The LIM homeodomain protein Lim-1 is widely expressed in neural, neural crest and mesoderm derivatives in vertebrate development. *Int. J. Dev. Biol.* **40**, 453-461.

Kiernan, A. E., Cordes, R., Kopan, R., Gossler, A. and Gridley, T. (2005). The Notch ligands DLL1 and JAG2 act synergistically to regulate hair cell development in the mammalian inner ear. *Development* **132**, 4353-4362.

Kobayashi, A., Kwan, K. M., Carroll, T. J., McMahon, A. P., Mendelsohn, C. L. and Behringer, R. R. (2005). Distinct and sequential tissue-specific activities of the LIM-class homeobox gene Lim1 for tubular morphogenesis during kidney development. *Development* **132**, 2809-2823.

Kopan, R. and Ilagan, M. X. G. (2004). g-Secretase: proteasome of the membrane? *Nat. Rev. Mol. Cell Biol.* **5**, 7-12.

Kraman, M. and McCright, B. (2005). Functional conservation of Notch1 and Notch2 intracellular domains. *FASEB J.* **19**, 1311-1313.

Kreidberg, J. A., Sariola, H., Loring, J. M., Maeda, M., Pelletier, J., Housman, D. and Jaenisch, R. (1993). WT-1 is required for early kidney development. *Cell* **74**, 679-691.

Laitinen, L., Virtanen, I. and Saxen, L. (1987). Changes in the glycosylation

pattern during embryonic development of mouse kidney as revealed with lectin conjugates. *J. Histochem. Cytochem.* **35**, 55-65.
Leimeister, C., Schumacher, N. and Gessler, M. (2003). Expression of Notch pathway genes in the embryonic mouse metanephros suggests a role in proximal tubule development. *Gene Expr. Patterns* **3**, 595-598.
Li, J., Chen, F. and Epstein, J. A. (2000). Neural crest expression of Cre recombinase directed by the proximal Pax3 promoter in transgenic mice. *Genesis* **26**, 162-164.
Li, L. H., Krantz, I. D., Deng, Y., Genin, A., Banta, A. B., Collins, C. C., Qi, M., Trask, B. J., Kuo, W. L., Cochran, J. et al. (1997). Alagille-syndrome is caused by mutations in human Jagged1, which encodes a ligand for Notch1. *Nat. Genet.* **16**, 243-251.
Lubman, O. Y., Korolev, S. V. and Kopan, R. (2004). Anchoring notch genetics and biochemistry; structural analysis of the ankyrin domain sheds light on existing data. *Mol. Cell* **13**, 619-626.
Lubman, O. Y., Kopan, R., Waksman, G. and Korolev, S. (2005). The crystal structure of a partial mouse Notch-1 ankyrin domain: repeats 4 through 7 preserve an ankyrin fold. *Protein Sci.* **14**, 1274-1251.
Lubman, O. Y., Ilagan, M. X., Kopan, R. and Barrick, D. (2007). Quantitative dissection of the Notch:CSL interaction: insights into the Notch-mediated transcriptional switch. *J. Mol. Biol.* **365**, 577-589.
McCright, B. (2003). Notch signaling in kidney development. *Curr. Opin. Nephrol. Hypertens.* **12**, 5-10.
McCright, B., Gao, X., Shen, L. Y., Lozier, J., Lan, Y., Maguire, M., Herzlinger, D., Weinmaster, G., Jiang, R. L. and Gridley, T. (2001). Defects in development of the kidney, heart and eye vasculature in mice homozygous for a hypomorphic Notch2 mutation. *Development* **128**, 491-502.
McDaniell, R., Warthen, D. M., Sanchez-Lara, P. A., Pai, A., Krantz, I. D., Piccoli, D. A. and Spinner, N. B. (2006). NOTCH2 mutations cause Alagille syndrome, a heterogeneous disorder of the notch signaling pathway. *Am. J. Hum. Genet.* **79**, 169-173.
Mumm, J. S. and Kopan, R. (2000). Notch signaling: from the outside in. *Dev. Biol.* **228**, 151-165.
Mundel, P., Heid, H. W., Mundel, T. M., Kruger, M., Reiser, J. and Kriz, W. (1997). Synaptopodin: an actin-associated protein in telencephalic dendrites and renal podocytes. *J. Cell Biol.* **139**, 193-204.
Murtaugh, L. C., Stanger, B. Z., Kwan, K. M. and Melton, D. A. (2003). Notch signaling controls multiple steps of pancreatic differentiation. *Proc. Natl. Acad. Sci. USA* **100**, 14920-14925.
Nakai, S., Sugitani, Y., Sato, H., Ito, S., Miura, Y., Ogawa, M., Nishi, M., Jishage, K., Minowa, O. and Noda, T. (2003). Crucial roles of Brn1 in distal tubule formation and function in mouse kidney. *Development* **130**, 4751-4759.
Nichols, A. M., Pan, Y., Herreman, A., Hadland, B. K., De Strooper, B., Kopan, R. and Huppert, S. (2004). The Notch pathway is dispensable for adipocyte specification. *Genesis* **40**, 40-44.
Ohyama, T. and Groves, A. K. (2004). Generation of Pax2-Cre mice by modification of a Pax2 bacterial artificial chromosome. *Genesis* **38**, 195-199.
Ong, C., Cheng, H., Chang, L. W., Ohtsuka, T., Kageyama, R., Stormo, D. G. and Kopan, R. (2006). Target selectivity of vertebrate Notch proteins: collaboration between discrete domains and CSL binding site architecture determine activation probability. *J. Biol. Chem.* **281**, 5106-5119.
Pan, Y., Lin, M., Tian, X., Cheng, H., Gridley, T., Shen, J. and Kopan, R. (2004). g-Secretase functions through Notch signaling to maintain skin appendages but is not required for their patterning or initial morphogenesis. *Dev. Cell* **7**, 731-743.
Perantoni, A. O., Timofeeva, O., Naillat, F., Richman, C., Pajni-Underwood, S., Wilson, C., Vainio, S., Dove, L. F. and Lewandoski, M. (2005). Inactivation of FGF8 in early mesoderm reveals an essential role in kidney development. *Development* **132**, 3859-3871.
Piccoli, D. A. and Spinner, N. B. (2001). Alagille syndrome and the Jagged1 gene. *Semin. Liver Dis.* **21**, 525-534.
Piscione, T. D., Wu, M. Y. and Quaggin, S. E. (2004). Expression of Hairy/Enhancer of Split genes, Hes1 and Hes5, during murine nephron morphogenesis. *Gene Expr. Patterns* **4**, 707-711.
Rogers, S. A., Ryan, G. and Hammerman, M. R. (1991). Insulin-like growth factors I and II are produced in the metanephros and are required for growth and development in vitro. *J. Cell Biol.* **113**, 1447-1453.
Ryan, G., Steele-Perkins, V., Morris, J. F., Rauscher, F. J., 3rd and Dressler, G. R. (1995). Repression of Pax-2 by WT1 during normal kidney development. *Development* **121**, 867-875.
Saxen, L. (1987). *Organogenesis of the Kidney*. Cambridge: Cambridge University Press.
Soriano, P. (1999). Generalized lacZ expression with the ROSA26 Cre reporter strain. *Nat. Genet.* **21**, 70-71.
Tanigaki, K., Han, H., Yamamoto, N., Tashiro, K., Ikegawa, M., Kuroda, K., Suzuki, A., Nakano, T. and Honjo, T. (2002). Notch-RBP-J signaling is involved in cell fate determination of marginal zone B cells. *Nat. Immunol.* **3**, 443-450.
Wang, P., Pereira, F. A., Beasley, D. and Zheng, H. (2003). Presenilins are required for the formation of comma- and S-shaped bodies during nephrogenesis. *Development* **130**, 5019-5029.
Welshons, W. J. (1958). The analysis of a pseudoallelic recessive lethal system at the notch locus of Drosophila melanogaster. *Cold Spring Harb. Symp. Quant. Biol.* **23**, 171-176.
Xu, P. X., Zheng, W., Huang, L., Maire, P., Laclef, C. and Silvius, D. (2003). Six1 is required for the early organogenesis of mammalian kidney. *Development* **130**, 3085-3094.